Literature review and discussions of inverse scattering series on internal multiple prediction

Jian Sun* and Kris Innanen*

ABSTRACT

Internal multiple attenuation is an increasingly high priority in seismic data analysis in the wake of increased sensitivity of primary amplitudes in quantitative interpretation, due to more information intend to be squeezed from seismic data. Removal of internal multiple is still a big challenge even though several various methods has been proposed. Inverse scattering series internal multiple attenuation algorithm, with great potential, developed by Weglein and collaborators in the 1990s, indicated that all internal multiples can be estimated by combining those sub-events satisfying a certain schema,which is the lower-higher-lower criterion. Many considerable discussions of internal multiple attenuation have been made based on inverse scattering series algorithm. In this paper, start with forward scattering series, we comprehensive review inverse scattering series internal multiple attenuation algorithm both in theoretical and its applications.

INTRODUCTION

Multiples attenuation and identification remains to be an indispensable procedure in seismic data processing and its quality will directly affect the accuracy of quantitative interpretation. When the influence of free-surface is considered, multiples can be identified as two major classes, surface-related multiple and interbed multiple. Due to its periodic characteristic in τ - p domain, surface-related multiples can be eliminated in a comfortable manner and many innovative technologies have been developed in different domains, such as predictive deconvolution (Taner, 1980), inverse approach using feedback model (Verschuur, 1991), embedding technique (Liu et al., 2000), inverse data processing (Berkhout and Verschuur, 2005; Berkhout, 2006; Ma et al., 2009). However, the attenuation of the other classical multiple, internal multiple, is still a giant challenge, especially on land data, even though much considerable progresses have been made recently.

Kelamis et al. (2002a,b) introduced a boundary-related/layer-related approach to remove internal multiples in the post-stack data (CMP domain). Berkhout and Verschuur (2005) extended the inverse data processing to attenuate internal multiples by considering them as the suppositional surface-related multiples through the boundary-related/layer-related approach in common-focus-point (CFP) domain. The same algorithm was applied by Luo et al. (2007) through re-datuming the top of the multiple generators and transforming internal multiples to be 'surface-related'. The common ground of those algorithms is that, as it were, extensive knowledge of subsurface is required;thus if the possibility exists that multiple removal will have to take place with incomplete knowledge of the velocity structure and generators, the ISS approach will be optimal.

By analysing the mechanical context of forward scattering series, Araujo et al. (1994)

*University of Calgary, CREWES Project

and Weglein et al. (1997, 2003) demonstrated that all possible internal multiples can be reconstructed, in an automatic way, as the combination of those sub-events satisfying a certain criterion, and the processing can be achieved by implementing the inverse scattering series in an appropriate manner. In this paper, to better understand the specification and innovative working mechanism of inverse scattering series internal multiple prediction algorithm, we retrospect its derivation procedure by beginning with forward scattering series.

BORN SERIES AND APPROXIMATION

Consider a 2D acoustic medium with constant density, the wave equation can be written as

$$\big[\nabla^2 + \frac{\omega^2}{c^2(\vec{\mathbf{r}})}\big]P(\vec{\mathbf{r}}|\vec{\mathbf{r}}_s,\omega) = \xi(\vec{\mathbf{r}}|\vec{\mathbf{r}}_s) \tag{1}$$

Scattering theorem delineates wave propagation in a real medium as the combination of a perturbation and the wavefield in a reference medium. Therefore, the spatially varying velocity $c(\vec{\mathbf{r}})$ can be rewritten into a reference velocity c_0 with a perturbation $a_c(\vec{\mathbf{r}})$,

$$\begin{aligned} \frac{1}{c^2(\vec{\mathbf{r}})} &= \frac{1}{c_0^2(\vec{\mathbf{r}})}[1 - a_c(\vec{\mathbf{r}})] \\ a_c(\vec{\mathbf{r}}) &= 1 - \frac{c_0^2(\vec{\mathbf{r}})}{c^2(\vec{\mathbf{r}})} \end{aligned} \tag{2}$$

where,$a_c(\vec{\mathbf{r}})$ is a dimensionless quantity, which varies as $c(\vec{\mathbf{r}})$ deviates from $c_0(\vec{\mathbf{r}})$.And applying this change into Eq.(1), we have,

$$\big[\nabla^2 + \frac{\omega^2}{c_0^2(\vec{\mathbf{r}})}\big]P(\vec{\mathbf{r}}|\vec{\mathbf{r}}_s,\omega) = \xi(\vec{\mathbf{r}}|\vec{\mathbf{r}}_s) + \frac{\omega^2}{c_0^2(\vec{\mathbf{r}})}a_c(\vec{\mathbf{r}})P(\vec{\mathbf{r}}|\vec{\mathbf{r}}_s) \tag{3}$$

Rewrite Eq.(1) and Eq.(3) into operator form,

$$\begin{aligned} &\mathfrak{L}(\vec{\mathbf{r}},\omega|c)P(\vec{\mathbf{r}}|\vec{\mathbf{r}}_s,\omega) = \xi(\vec{\mathbf{r}}|\vec{\mathbf{r}}_s) \\ &\mathfrak{L}_0(\vec{\mathbf{r}},\omega|c)P(\vec{\mathbf{r}}|\vec{\mathbf{r}}_s,\omega) = \xi(\vec{\mathbf{r}}|\vec{\mathbf{r}}_s) + V(\vec{\mathbf{r}},\omega)P(\vec{\mathbf{r}}|\vec{\mathbf{r}}_s,\omega) \end{aligned} \tag{4}$$

Here, $V(\vec{\mathbf{r}},\omega)$ is the scattering potential at $\vec{\mathbf{r}}$, and can be expressed as,

$$V(\vec{\mathbf{r}},\omega) = \mathfrak{L}(\vec{\mathbf{r}},\omega|c) - \mathfrak{L}_0(\vec{\mathbf{r}},\omega|c) = \frac{\omega^2}{c_0^2(\vec{\mathbf{r}})}a_c(\vec{\mathbf{r}}) \tag{5}$$

Lippmann-Schwinger equation can be acquired based on divergence theorem,

$$G(\vec{\mathbf{r}}|\vec{\mathbf{r}}_s,\omega) = G_0(\vec{\mathbf{r}}|\vec{\mathbf{r}}_s,\omega) + \int_{-\infty}^{+\infty} G_0(\vec{\mathbf{r}}|\vec{\mathbf{r}}',\omega)\frac{\omega^2}{c_0^2(\vec{\mathbf{r}}')}a_c(\vec{\mathbf{r}}')G(\vec{\mathbf{r}}'|\vec{\mathbf{r}}_s,\omega)\mathrm{d}\vec{\mathbf{r}}' \tag{6}$$

And its matrix notion, where we have *born series*,

$$\boldsymbol{G} = \boldsymbol{G}_0 + \boldsymbol{G}_0\boldsymbol{V}\boldsymbol{G} \tag{7a}$$

$$\boldsymbol{G} = \boldsymbol{G}_0 + \boldsymbol{G}_0\boldsymbol{V}\boldsymbol{G}_0 + \boldsymbol{G}_0\boldsymbol{V}\boldsymbol{G}_0\boldsymbol{V}\boldsymbol{G}_0 + \boldsymbol{G}_0\boldsymbol{V}\boldsymbol{G}_0\boldsymbol{V}\boldsymbol{G}_0\boldsymbol{V}\boldsymbol{G}_0 + \dots \tag{7b}$$

An infinite series 7b can be reached if the $\boldsymbol{G}$ is substituted by the right-hand-side of Eq.(7a). Eq.(7b) shows that the wave propagation in a real medium can be represented as an infinite sum of terms sorted by orders of scattering potential in a reference medium (Figure 1), where $\boldsymbol{G}_0$ describes the zeros order of perturbation, i.e., the direct wave in a reference medium; $\boldsymbol{G}_0\boldsymbol{V}\boldsymbol{G}_0$ stands for wave propagation in a reference medium through one perturbation, and so on. *Born approximation* is reached if only the series was truncated by first order of Eq.(7b),

$$G(\vec{\mathbf{r}}|\vec{\mathbf{r}}_s,\omega) = G_0(\vec{\mathbf{r}}|\vec{\mathbf{r}}_s,\omega) + \int_{-\infty}^{+\infty} G_0(\vec{\mathbf{r}}|\vec{\mathbf{r}}',\omega)V(\vec{\mathbf{r}},\omega)G_0(\vec{\mathbf{r}}'|\vec{\mathbf{r}}_s,\omega)\mathrm{d}\vec{\mathbf{r}}' \tag{8}$$

Analogously, 2D *Born approximation* can be written as,

$$\begin{aligned} G(x_g,z_g,x_s,z_s,\omega) = {} & G_0(x_g,z_g,x_s,z_s,\omega) \\ & + \iint_{-\infty}^{+\infty} G_0(x_g,z_g,x_1,z_1,\omega)V(x_1,z_1)G_0(x_1,z_1,x_s,z_s,\omega)\mathrm{d}x_1\mathrm{d}z_1 \end{aligned} \tag{9}$$

By understanding the mechanism of forward scattering series, based on the fact of that, primaries and multiples are related to the order of perturbation, i.e., 1st order internal multiples have at least three perturbations which satisfy lower-higher-lower relationship in depth, 2nd-order internal multiples have at least five perturbations, and so on. Therefore, leading-order internal multiple prediction algorithm can be derived by inverse scattering series on strength of the order of perturbation.

INTRODUCTION OF INVERSE SCATTERING SERIES

Green's Function

1D scalar Green's function in an acoustic homogeneous medium with constant density,

$$G_0(z_g,z_s,\omega) = \frac{e^{\mathrm{i}k|z_g-z_s|}}{\mathrm{i}2k}, k = \frac{\omega}{c_0} \tag{10}$$

And 2D Green's Function in the reference medium (homogeneous and acoustic with constant ρ) can be obtained using Weyl-integral,

$$G_0(x_g,z_g,x_s,z_s,\omega) = \frac{1}{2\pi}\int_{-\infty}^{+\infty} \frac{e^{\mathrm{i}k_s(x_g-x_s)}e^{\mathrm{i}\nu_s|z_g-z_s|}}{\mathrm{i}2\nu_s}\mathrm{d}k_s \tag{11}$$

with

$$\nu_s = \sqrt{\frac{\omega^2}{c_0^2} - k_s^2}$$

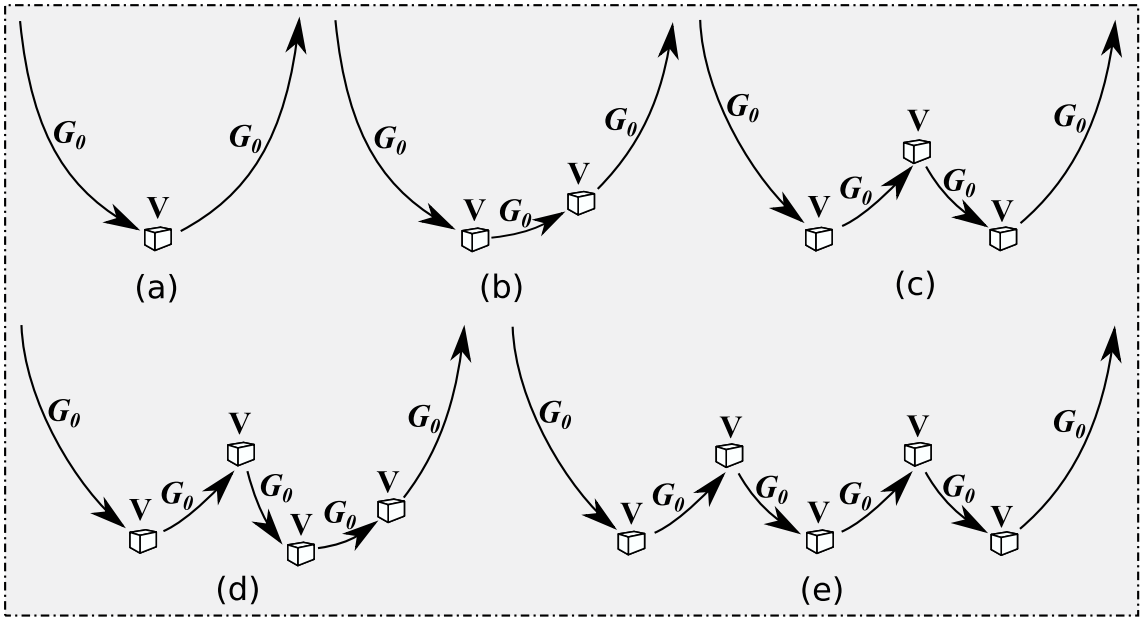

FIG. 1. Wave propagation in perturbation mode.

Rewrite 2D Green's Function as,

$$G_0(x_g, z_g, x_s, z_s, \omega) = \frac{1}{2\pi}\int_{-\infty}^{+\infty} \frac{e^{-\mathrm{i}k_s x_s}}{\mathrm{i}2\nu_s}\phi_0(x_g, z_g, k_s, z_s, \omega)\mathrm{d}k_s \tag{12}$$

where,

$$\phi_0(x_g, z_g, k_s, z_s, \omega) = e^{\mathrm{i}(k_s x_g + \nu_s|z_g - z_s|)} \tag{13}$$

which means, $G_0(x_g, z_g, x_s, z_s, \omega)$ is the inverse Fourier transform of $\frac{1}{\mathrm{i}2\nu_s}\phi_0(x_g, z_g, k_s, z_s, \omega)$ with respect to k_s. Rewrite Eq.(12) into wavenumber domain, we have, $\phi_0(x_g, z_g, k_s, z_s, \omega) = \mathrm{i}2\nu_s G_0(x_g, z_g, k_s, z_s, \omega)$. In other words, the 2D Green's Function can be delineated as a superposition of weighted plane wave solution.

Therefore, if we interpret Eq.(7b) in source-wavenumber domain, i.e., taking Fourier transform of it on both sides, with respect to x_s, and then multiplying by $\mathrm{i}2\nu_s$ gives,

$$\begin{aligned}
&\mathrm{i}2\nu_s \boldsymbol{G}(x_g, z_g, k_s, z_s, \omega) \\
&= \mathrm{i}2\nu_s \boldsymbol{G}_0(x_g, z_g, k_s, z_s, \omega) + \boldsymbol{G}_0(x_g, z_g, x_1, z_1, \omega)\boldsymbol{V}(x_1, z_1)\mathrm{i}2\nu_s \boldsymbol{G}_0(x_1, z_1, k_s, z_s, \omega) \\
&+ \boldsymbol{G}_0(x_g, z_g, x_1, z_1, \omega)\boldsymbol{V}(x_1, z_1)\boldsymbol{G}_0(x_1, z_1, x_2, z_2, \omega)\boldsymbol{V}(x_2, z_2)\mathrm{i}2\nu_s \boldsymbol{G}_0(x_2, z_2, k_s, z_s, \omega) \\
&+ \ldots
\end{aligned} \tag{14}$$

Again, combining with Eq.(12), it can be written in matrix notation as,

$$\boldsymbol{\phi} = \boldsymbol{\phi}_0 + \boldsymbol{G}_0\boldsymbol{V}\boldsymbol{\phi}_0 + \boldsymbol{G}_0\boldsymbol{V}\boldsymbol{G}_0\boldsymbol{V}\boldsymbol{\phi}_0 + \boldsymbol{G}_0\boldsymbol{V}\boldsymbol{G}_0\boldsymbol{V}\boldsymbol{G}_0\boldsymbol{V}\boldsymbol{\phi}_0 + \ldots \tag{15}$$

Inverse scattering series

Based on Eq.(15), the scattered wavefield of an incident plane wave is expressed as,

$$\boldsymbol{b}_1 = \boldsymbol{\phi} - \boldsymbol{\phi}_0 = \boldsymbol{G}_0\boldsymbol{V}\boldsymbol{\phi}_0 + \boldsymbol{G}_0\boldsymbol{V}\boldsymbol{G}_0\boldsymbol{V}\boldsymbol{\phi}_0 + \boldsymbol{G}_0\boldsymbol{V}\boldsymbol{G}_0\boldsymbol{V}\boldsymbol{G}_0\boldsymbol{V}\boldsymbol{\phi}_0 + \ldots \tag{16}$$

Here,$\boldsymbol{b}_1 = \mathrm{i}2\nu_s(\boldsymbol{G} - \boldsymbol{G}_0) = \mathrm{i}2\nu_s\boldsymbol{D}$ is the weighted scattered wavefield of point sources, and $\boldsymbol{D}(z_g, z_s, \omega)$ is the measured data on surface without direct wave.

And split scattering potential V into series by orders,

$$\boldsymbol{V} = \boldsymbol{V}_1 + \boldsymbol{V}_2 + \boldsymbol{V}_3 + \dots \tag{17}$$

Substitute this change into scattering wavefield representation (Eq.16), and equate like orders, we have,

$$\begin{aligned}
\boldsymbol{b}_1 &= \boldsymbol{G}_0\boldsymbol{V}_1\boldsymbol{\phi}_0, && \text{(18a)}\\
\boldsymbol{0} &= \boldsymbol{G}_0\boldsymbol{V}_2\boldsymbol{\phi}_0 + \boldsymbol{G}_0\boldsymbol{V}_1\boldsymbol{G}_0\boldsymbol{V}_1\boldsymbol{\phi}_0, && \text{(18b)}\\
\boldsymbol{0} &= \boldsymbol{G}_0\boldsymbol{V}_3\boldsymbol{\phi}_0 + \boldsymbol{G}_0\boldsymbol{V}_2\boldsymbol{G}_0\boldsymbol{V}_1\boldsymbol{\phi}_0 + \boldsymbol{G}_0\boldsymbol{V}_1\boldsymbol{G}_0\boldsymbol{V}_2\boldsymbol{\phi}_0 + \boldsymbol{G}_0\boldsymbol{V}_1\boldsymbol{G}_0\boldsymbol{V}_1\boldsymbol{G}_0\boldsymbol{V}_1\boldsymbol{\phi}_0, && \text{(18c)}\\
&\vdots
\end{aligned}$$

By solving those series reversion, the certain order of scattering potential term can be obtained in terms of weighted measured data $\boldsymbol{b}_1(z_g, z_s, t)$. In next section, we show how to interpret the internal multiple in a certain order of perturbation in both 1D and 2D.

INTERNAL MULTIPLE PREDICTION ALGORITHM

Internal multiples prediction (IMs) algorithm based on inverse scattering series (ISS) was first introduced in wavenumber-pseudo depth domain by Araujo et al. (1994) and Weglein et al. (1997). Thereafter, Coates and Weglein (1996) demonstrated that the algorithm can also be implemented in $\tau - p$ domain. In this section, we take 1D acoustic medium as an example to show the derivation of IMs prediction algorithm in pseudo-depth domain. Based on the monotonicity relation between pseudo-depth and intercept time for acoustic medium, the plane wave domain ISS-IMs prediction algorithm is introduced in the upcoming section. Beyond that, to involve the non-stationary search parameters, the time domain ISS-IMs prediction algorithm proposed by Innanen (2016a) is also demonstrated in the following context.

ISS-IMs prediction algorithm in pseudo-depth domain

Consider 1D acoustic medium (reference is homogeneous), and replacing 1D Green function (Eq.10) in the first-order equation of inverse scattering series (Eq.18a),

$$\begin{aligned}
b_1(z_g, z_s, \omega) &= \int_{-\infty}^{+\infty} G_0(z_g, z_1, \omega)V_1(z_1)\phi_0(z_1, z_s, \omega)\mathrm{d}z_1\\
&= \int_{-\infty}^{+\infty} \frac{e^{\mathrm{i}k_0|z_g - z_1|}}{\mathrm{i}2k_0}V_1(z_1)e^{\mathrm{i}k_0|z_1 - z_s|}\mathrm{d}z_1\\
&= \frac{e^{-\mathrm{i}k_0(z_g + z_s)}}{\mathrm{i}2k_0}\int_{-\infty}^{+\infty} e^{\mathrm{i}2k_0 z_1}V_1(z_1)\mathrm{d}z_1\\
&= \frac{e^{-\mathrm{i}k_0(z_g + z_s)}}{\mathrm{i}2k_0}V_1(2k_0)
\end{aligned} \tag{19}$$

Therefore, the 1st-order of scattering potential can be written in terms of weighted measured data,

$$V_1(2k_0) = \mathrm{i}2k_0 e^{\mathrm{i}k_0(z_g+z_s)} b_1(z_g, z_s, k_0) \tag{20}$$

where $k_0 = \dfrac{\omega}{c_0}$.

The 1st-order internal multiple can be generated at least 3 perturbations which satisfy lower-higher-lower relationship in pseudo-depth (depth in reference medium). By analyzing 3rd order in inverse scattering series (Eq.18c), we have,

$$\begin{aligned} \boldsymbol{G}_0\boldsymbol{V}_3\boldsymbol{\phi}_0 &= -(\boldsymbol{G}_0\boldsymbol{V}_2\boldsymbol{G}_0\boldsymbol{V}_1\boldsymbol{\phi}_0 + \boldsymbol{G}_0\boldsymbol{V}_1\boldsymbol{G}_0\boldsymbol{V}_2\boldsymbol{\phi}_0 + \boldsymbol{G}_0\boldsymbol{V}_1\boldsymbol{G}_0\boldsymbol{V}_1\boldsymbol{G}_0\boldsymbol{V}_1\boldsymbol{\phi}_0) \\ &= \boldsymbol{G}_0\boldsymbol{V}_{31}\boldsymbol{\phi}_0 + \boldsymbol{G}_0\boldsymbol{V}_{32}\boldsymbol{\phi}_0 + \boldsymbol{G}_0\boldsymbol{V}_{33}\boldsymbol{\phi}_0 \end{aligned} \tag{21}$$

The first two terms in 3rd-order have no contribution to internal multiple (they only contribute to primary energy, see analysis discussed by Araujo et al. (1994)). The 3rd term $\boldsymbol{G}_0\boldsymbol{V}_{33}\boldsymbol{\phi}_0$ represents several different wave propagations through three perturbations depending on the variant depth relations between perturbations (Figure 2).

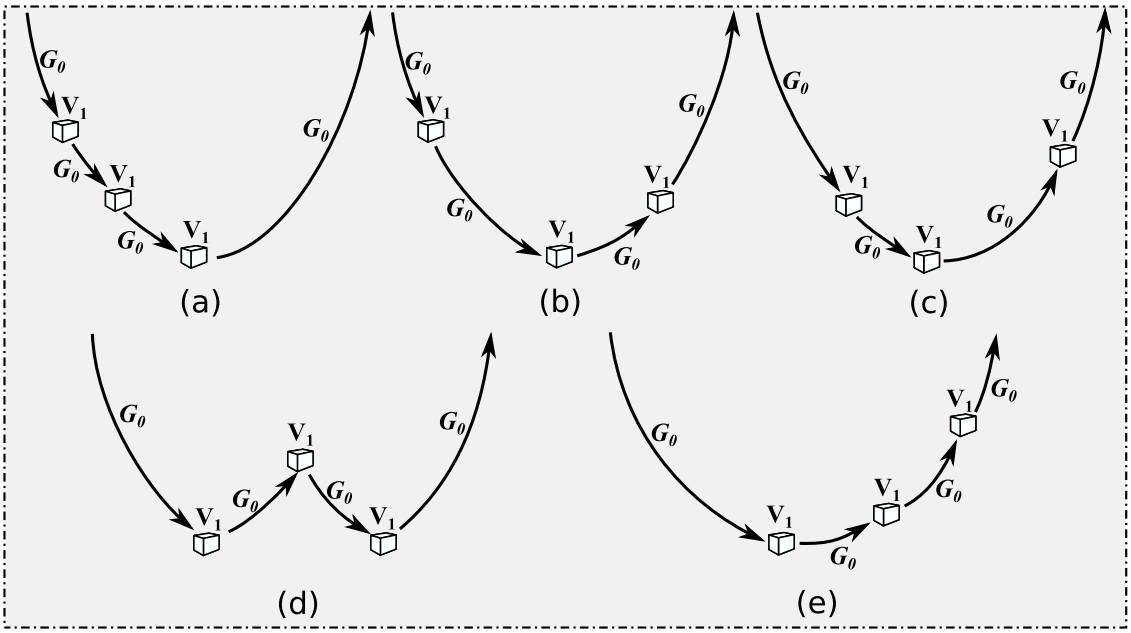

FIG. 2. Contributions of $\boldsymbol{G}_0\boldsymbol{V}_{33}\boldsymbol{G}_0$ depending on variant depth relations between perturbations. (a) case of $z_1 < z_2 < z_3$, (b) case of $z_1 < z_3 < z_2$, (c) case of $z_3 < z_1 < z_2$, (d) case of $z2 < z_1$ and $z_2 < z_3$, (e) case of $z_3 < z_2 < z_1$.

Consider all possible wave propagations involved by $\boldsymbol{G}_0\boldsymbol{V}_{33}\boldsymbol{\phi}_0$, only one certain wave path, with perturbations satisfying lower-higher-lower relationship in pseudo-depth, has contribution to 1st-order internal multiples, shown in Figure 2d, can be expressed as,

$$
\begin{aligned}
&W_{33}(z_g, z_s, \omega) \\
&= -\int_{-\infty}^{+\infty} \boldsymbol{G}_0(z_g, z_1, \omega) V_1(z_1) \mathrm{d}z_1 \int_{-\infty}^{z_1} \boldsymbol{G}_0(z_1, z_2, \omega) V_1(z_2) \mathrm{d}z_2 \\
&\quad \times \int_{z_2}^{+\infty} \boldsymbol{G}_0(z_2, z_3, \omega) V_1(z_3) \phi_0(z_3, z_s, \omega) \mathrm{d}z_3 \\
&= -\int_{-\infty}^{+\infty} \frac{e^{\mathrm{i}k_0|z_g - z_1|}}{\mathrm{i}2k_0} V_1(z_1) \mathrm{d}z_1 \int_{-\infty}^{z_1} \frac{e^{\mathrm{i}k_0|z_1 - z_2|}}{\mathrm{i}2k_0} V_1(z_2) \mathrm{d}z_2 \\
&\quad \times \int_{z_2}^{+\infty} \frac{e^{\mathrm{i}k_0|z_2 - z_3|}}{\mathrm{i}2k_0} V_1(z_3) e^{\mathrm{i}k_0|z_3 - z_s|} \mathrm{d}z_3 \\
&= -\frac{e^{-\mathrm{i}k_0(z_g + z_s)}}{\mathrm{i}2{k_0}^3} \int_{-\infty}^{+\infty} e^{\mathrm{i}2k_0 z_1} V_1(z_1) \mathrm{d}z_1 \int_{-\infty}^{z_1} e^{-\mathrm{i}2k_0 z_2} V_1(z_2) \mathrm{d}z_2 \int_{z_2}^{+\infty} e^{\mathrm{i}2k_0 z_3} V_1(z_3) \mathrm{d}z_3 \\
&= -\frac{e^{-\mathrm{i}k_0(z_g + z_s)}}{(\mathrm{i}2k_0)^3} V_1(2k_0|z_1) V_1(-2k_0|z_2 < z_1) V_1(2k_0|z_3 > z_2)
\end{aligned}
\tag{22}
$$

Substitute Eq.(20) into Eq.(22) to replace scattering potential V_1 by weighted measured data,

$$
W_{33}(z_g, z_s, \omega) = -b_1(z_g, z_s, k_0|z_1) b_1(z_g, z_s, -k_0|z_2 < z_1) b_1(z_g, z_s, k_0|z_3 > z_2) \tag{23}
$$

Inverse Fourier transform of $b_1(z_g, z_s, k_0)$ over k_0, all 1st-order internal multiples can be obtained by weighted measured data,

$$
\begin{aligned}
b_3(z_g, z_s, \omega) = &-\int_{-\infty}^{+\infty} e^{\mathrm{i}k_0 z_1} b_1(z_g, z_s, z_1) \mathrm{d}z_1 \int_{-\infty}^{z_1 - \epsilon} e^{-\mathrm{i}k_0 z_2} b_1(z_g, z_s, z_2) \mathrm{d}z_2 \\
&\times \int_{z_2 + \epsilon}^{+\infty} e^{\mathrm{i}k_0 z_3} b_1(z_g, z_s, z_3) \mathrm{d}z_3
\end{aligned}
\tag{24}
$$

Here, $b_1(z_g, z_s, \omega) = \mathrm{i}2k_0 D(z_g, z_s, \omega)$, $k_0 = \dfrac{\omega}{c_0}$, and $z_1 > z_2 < z_3$ are pseudo-depth, which can be calculated as $z = \dfrac{c_0 t}{2}$. Depending on the monotonicity condition analysis of pseudo-depth (Weglein et al., 2003; Nita and Weglein, 2009), it has the same interrelations as the real depth does.

Analogously, the 2nd-order internal multiple has at least 5 perturbations, which can be contributed by $\boldsymbol{G}_0\boldsymbol{V}_1\boldsymbol{G}_0\boldsymbol{V}_1\boldsymbol{G}_0\boldsymbol{V}_1\boldsymbol{G}_0\boldsymbol{V}_1\boldsymbol{G}_0\boldsymbol{V}_1\boldsymbol{\phi}_0$ if depth of perturbations meet the needs of 'lower-higher-lower' criterion.

The mathematical formula of 2D leading order internal multiple prediction algorithm based on inverse scattering series was demonstrated by Araujo et al. (1994) and Weglein

et al. (1997, 2003), written as,

$$b_3(k_g,k_s,\omega) = -\frac{1}{(2\pi)^2}\iint_{-\infty}^{+\infty} \mathrm{d}k_1\mathrm{d}k_2 e^{\mathrm{i}\nu_1(z_s-z_g)} e^{\mathrm{i}\nu_2(z_g-z_s)} \int_{-\infty}^{+\infty} \mathrm{d}z_1 e^{\mathrm{i}(\nu_1+\nu_g)z_1} b_1(k_g,k_1,z_1) \times \int_{-\infty}^{z_1-\epsilon} \mathrm{d}z_2 e^{-\mathrm{i}(\nu_2+\nu_1)z_2} b_1(k_1,k_2,z_2) \int_{z_2+\epsilon}^{+\infty} \mathrm{d}z_3 e^{\mathrm{i}(\nu_s+\nu_2)z_3} b_1(k_2,k_s,z_3) \tag{25}$$

where, the input is obtained by $b_1(k_g,k_s,z) = -i2\nu_s D(k_g,k_s,z)$. Relations between k_g, k_s, k_1, k_2 is interpreted in Figure 3, and ν_X is the vertical wavenumber, can be calculated as,

$$\nu_X = \sqrt{\frac{\omega^2}{c_0^2} - k_X^2}$$

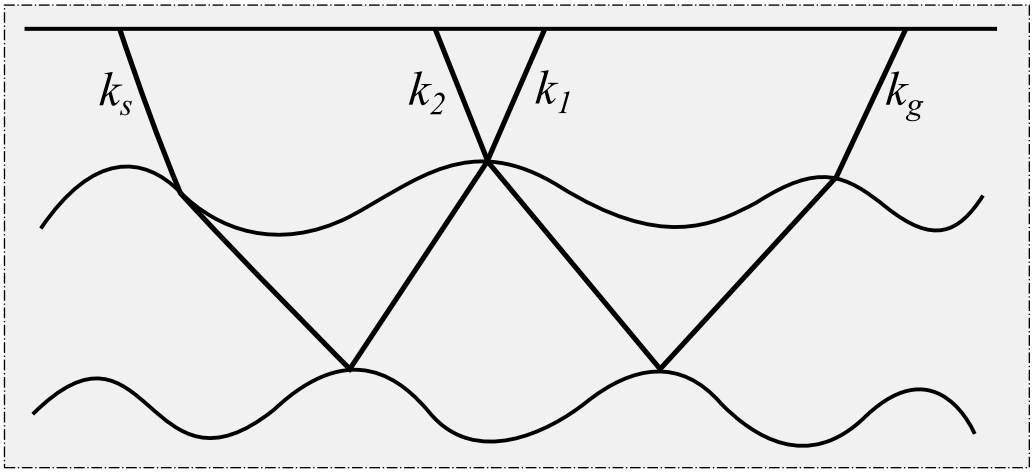

FIG. 3. Wavenumber relations in sub-events combination of generating internal multiples

ISS-IMs prediction algorithm in $\tau - p$ domain

The monotonicity requirements of pseudo-depth and intercept time in inverse scattering series for internal multiple prediction was first discussed by Nita and Weglein (2009) and further analyzed by Sun and Innanen (2015). Based on the fact of that, for acoustic media, the pseudo-depth has the unique projection on intercept time. In other words, the inverse scattering series internal multiple prediction algorithm also works in plane wave domain as long as sub-events in combination satisfy the 'longer-shorter-longer' relationship in intercept time.

The relation between pseudo-depth and intercept time in a reference media is written as,

$$k_z z = \omega\tau \tag{26}$$

where, $k_z = q_g + q_s$, z is the pseudo-depth, and τ is the intercept time.

Reconsider the IMs-ISS prediction algorithm in pseudo-depth domain Eq. (25), replacing the pseudo-depth (z) with intercept time (τ), and changing the wavenumber (k) into

horizontal slowness (p), the IMs-ISS prediction algorithm in plane wave domain can be reached, which was first mentioned by Coates and Weglein (1996), written as (See the completed derivation of plane wave domain 2D ISS-IMs prediction algorithm in Appendix A),

$$b_3(p_g,p_s,\omega) = -\frac{1}{(2\pi)^2}\iint_{-\infty}^{+\infty} \mathrm{d}p_1\mathrm{d}p_2 e^{\mathrm{i}q_1(\tau_s-\tau_g)} e^{\mathrm{i}q_2(\tau_g-\tau_s)} \int_{-\infty}^{+\infty} \mathrm{d}\tau_1 e^{\mathrm{i}\omega\tau_1} \boldsymbol{b}_1(p_g,p_1,\tau_1) \\ \times \int_{-\infty}^{\tau_1-\epsilon} \mathrm{d}\tau_2 e^{-\mathrm{i}\omega\tau_2} \boldsymbol{b}_1(p_1,p_2,\tau_2) \int_{\tau_2+\epsilon}^{+\infty} \mathrm{d}\tau_3 e^{\mathrm{i}\omega\tau_3} \boldsymbol{b}_1(p_2,p_s,\tau_3) \tag{27}$$

where, the input is the weighted measured data shown as $b_1(p_g,p_s,\tau) = -i2\omega q_s D(p_g,p_s,\tau)$, and q_X is the vertical slowness, can be calculated as,

$$q_X = \sqrt{\frac{1}{c_0^2} - p_X^2}$$

Another way to understand the plane wave domain ISS-IMs prediction algorithm, is that we achieve the horizontal slowness- pseudo depth (p,z) domain algorithm by replacing the wavenumber k with horizontal slowness p,

$$b_3(p_g,p_s,\omega) = -\frac{1}{(2\pi)^2}\iint_{-\infty}^{+\infty} \mathrm{d}p_1\mathrm{d}p_2 e^{\mathrm{i}\nu_1(z_s-z_g)} e^{\mathrm{i}\nu_2(z_g-z_s)} \int_{-\infty}^{+\infty} \mathrm{d}z_1 e^{\mathrm{i}(\nu_1+\nu_g)z_1} \boldsymbol{b}_1(p_g,p_1,z_1) \\ \times \int_{-\infty}^{z_1-\epsilon} \mathrm{d}z_2 e^{-\mathrm{i}(\nu_2+\nu_1)z_2} \boldsymbol{b}_1(p_1,p_2,z_2) \int_{z_2+\epsilon}^{+\infty} \mathrm{d}z_3 e^{\mathrm{i}(\nu_s+\nu_2)z_3} \boldsymbol{b}_1(p_2,p_s,z_3) \tag{27*}$$

And then, in reference medium, the pseudo-depth z can be easily transformed into the vertical travel time.

ISS-IMs prediction algorithm in time-offset domain

The intention of re-formulating the ISS-IMs attenuation in time-offset domain is originated from seeking a non-stationary search parameter to identify the lower-higher-lower criterion. In practical, wavelet in involved in seismic traces. The damaging artifacts would be introduced if the satisfaction of lower-higher-lower relation occurred within a wavelength, i.e., the depth/time range of one-event. Therefore, a search parameter (ϵ) has to be intervened to meet the lower-higher-lower relationship. Digging further, events are usually interfered with each other in a complex case involving many thin layers. In view of that, inverse scattering series internal multiple attenuation algorithm with a non-stationary data-driven search parameter becomes an impending problem. In the following context, we introduce the time-offset domain ISS-IMs prediction algorithm, re-formulated by Innanen (2016a,b) based on standard version of ISS-IMs prediction algorithm in pseudo-depth domain.

Consider source and receivers are located on the surface (i.e., $z_g = z_s = 0$), and assume under-earth strata are layered ($k_g = k_s$), 1.5D version of ISS-IMs attenuation algorithm in

pseudo-depth domain can be reached,

$$b_3(k_g,\omega)=\int_{-\infty}^{+\infty}e^{\mathrm{i}k_z z_1}\boldsymbol{b}_1(k_g,z_1)\mathrm{d}z_1\int_{-\infty}^{z_1-\epsilon_1}e^{-\mathrm{i}k_z z_2}\boldsymbol{b}_1(k_g,z_2)\mathrm{d}z_2\int_{z_2+\epsilon_2}^{+\infty}e^{\mathrm{i}k_z z_3}\boldsymbol{b}_1(k_g,z_3)\mathrm{d}z_3 \tag{28}$$

If we only focus on the arrival times of internal multiple prediction, i.e., neglect the weight, and replacing the input $b_1(k_g,z)$ by the Fourier transform of unweighted data $d(x_g,t)$ with respect to x_g, denoted by $D(k_g,t)$,

$$b_{IM3}(k_g,\omega)=\int_{-\infty}^{+\infty}e^{\mathrm{i}\omega t}\boldsymbol{D}(k_g,t_1)\mathrm{d}t_1\int_{-\infty}^{t_1-\epsilon_1}e^{-\mathrm{i}\omega t_2}\boldsymbol{D}(k_g,t_2)\mathrm{d}t_2\int_{t_2+\epsilon_2}^{+\infty}e^{\mathrm{i}\omega t_3}\boldsymbol{D}(k_g,t_3)\mathrm{d}t_3 \tag{29}$$

Note that, $k_z z$ was substituted by ωt, which is legitimate only if the ordering of sub-events in total traveltime t is the same as ordering in vertical traveltime τ (Nita and Weglein, 2009) (Intercept time τ has the same monotonicity condition as the real depth does, see in Appendix). As noted above, the non-stationary search parameter works for $\tau-p$ domain as well as the time-offset domain.

Change the output domain into (k_g,t) and replacing the products of integrals over time by modified convolutions and correlations, the Eq. 29 can be re-written as,

$$\boldsymbol{B}_{IM3}(k_g,t)=\int_{-\infty}^{+\infty}\mathrm{d}t_1\boldsymbol{D}(k_g,t_1-t)\int_{\alpha(t,t_1)}^{\beta(t)}\mathrm{d}t_2\boldsymbol{D}(k_g,t_1-t_2)\boldsymbol{D}(k_g,t_2) \tag{30}$$

where,

$$\begin{aligned}\alpha(t,t_1)&=t_1-(t-\epsilon_2)\\ \beta(t)&=t-\epsilon_1\end{aligned} \tag{31}$$

The remaining products in wavenumber k_g can also be substituted by the convolution in space x, to transform the output into time-offset domain, Eq. 31 becomes as,

$$\boldsymbol{IM}_3(x,t)=\int\mathrm{d}x_1\int\mathrm{d}t_1\boldsymbol{d}(x-x_1,t_1-t)\int\mathrm{d}x_2\int_{\alpha(t,t_1)}^{\beta(t)}\mathrm{d}t_2\boldsymbol{d}(x_1-x_2,t_1-t_2)\boldsymbol{d}(x_2,t_2) \tag{32}$$

By laying $k_g=k_s=0$, the case reduces to 1D normal incidence, with time-domain form of the prediction,

$$\boldsymbol{IM}_3(t)=\int_{-\infty}^{+\infty}\mathrm{d}t_1\boldsymbol{D}(t_1-t)\int_{\alpha(t,t_1)}^{\beta(t)}\mathrm{d}t_2\boldsymbol{D}(t_1-t_2)\boldsymbol{D}(t_2) \tag{33}$$

IMPLEMENTATION OF ISS-IM PREDICTION AND WHICH DOMAIN

Many incentive research and discussions of inverse scattering series on internal multiple attenuation have been made depending on the variant purposes, (1) correcting predicted

amplitude of internal multiples (Zou and Weglein, 2015), and (2) refining the algorithm for certain high priority acquisition styles and environments, since it was developed by Weglein and collaborators in 1990s. Hernandez and Innanen (2014) examined the possibility of containing the amplitude energy by implementing 1D ISS-IMs prediction algorithm in pseudo-depth domain on both physical modeling and post-stack land data. The application of 1.5D ISS-IMs prediction algorithm was also carried out on physical modeling data in pseudo-depth domain (Pan et al., 2014; Pan and Innanen, 2015; Pan, 2015).

The difficulties of successfully implementing ISS-IMs prediction algorithm arise on land data due to its unique complex features such as noisy, poor coupling, multi-thin bedding, in-completed geometry spreading (Luo et al., 2011; Wu et al., 2011; de Melo et al., 2014). However, the precise internal multiple removal remains favorite problems on land because of the high sensitivity requirement of inversion and interpretation. Therefore, any possible impacts, investigations and discussion in precision of internal multiple prediction are incentive for land.

Search parameter

One reason, increasing the trouble of land ISS-IMs prediction, is that the previous noted limitations integrate sub-events uncertainly in the combination of internal multiple prediction (Weglein and Matson, 1998). A key ingredient of separation of sub-events, either in pseudo-depth or in intercept time, is the search parameter applied in prediction algorithm (Hernandez and Innanen, 2014), and its importance was first mentioned by Coates and Weglein (1996). A fixed search parameter was first introduced in a standard version of pseudo-depth domain ISS-IMs prediction algorithm developed by Weglein et al. (1997, 2003). However, the data combination are not always linear in ISS-IMs prediction which leads to large dip artifacts occurred in predicted results using a fixed search parameter. To solve this and enhance the precision of internal multiple prediction, two lines can be thought out, (1) seeking for a non-stationary search parameter, (2) optimize the prediction algorithm to implement it in stationary ϵ way.

As illustrated in Figure 4a, the input $b_1(k_g, z)$ becomes to be dispersed as wavenumber k_g increasing. In other words, inverse scattering series prediction with a small fixed search parameter will consider one event as two or more sub-events at large wavenumber k_g, which produces, what we called, high angle artifacts (Figure 5). Conversely, the prediction, with a large fixed value for ϵ, will miss some of proper combinations and leads to an uncompleted estimation.

To mitigate those artifacts related to a small fixed ϵ, for 1.5D case, instead of using a fixed value for ϵ, Innanen and Pan (2015) proposed an approximated variant search parameter (ϵ), as a linear function of k_g (See in Figure 6). However, the approximate linear $\epsilon(k_g)$ encounters big challenges when the overlap occurred between sub-events in combination due to the dispersion of input at high angle (large k_g), which is frequently happening in land.

Digging further, by following the 1st-line, the time domain prediction algorithm with a non-stationary ϵ was refined by Innanen (2016b), when the total traveltime is a monotonic

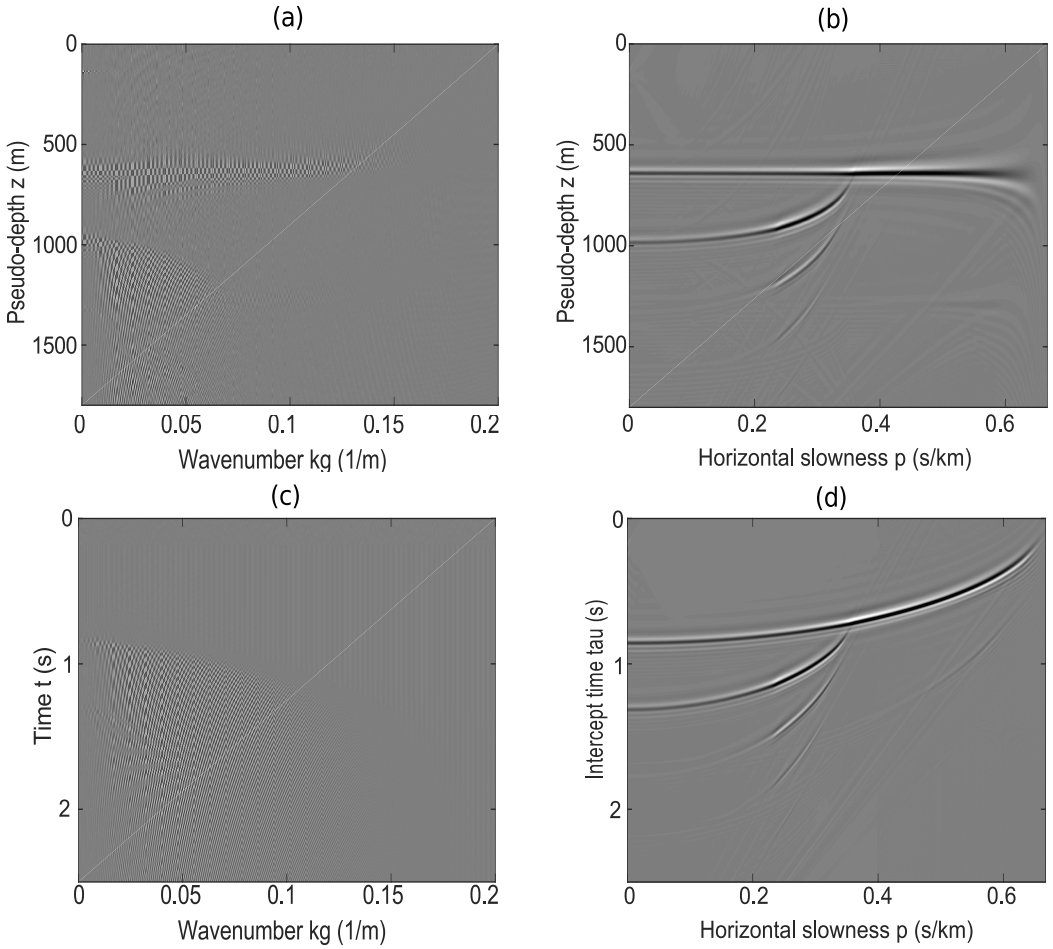

FIG. 4. The distribution of various input data. (a) $b_1(k_g, z)$; (b) $b_1(p_g, z)$; (c) $b_1(k_g, t)$; (d) $b_1(p_g, \tau)$.

function of real depth. In Figure 4c, the input $b_1(k_g, t)$ shows a similar distribution as in wavenumber-pseudo depth domain $b_1(k_g, z)$. However, time domain algorithm (Eq. 30) allows a non-stationary ϵ which is not involved in pseudo-depth domain. More details and discussions of non-stationary parameter can be found by Innanen (2016a), and time-offset domain input is not shown here due to time consuming.

Take the second observation into Figure 4c, the search parameter is high correlated to convergence of input. Which means search parameter will be easier to be prepared, even for non-stationary, if the input is more concentrated. Change wavenumber into horizontal slowness, the input $b_1(p_g, z)$, shown in Figure 4b, is prepared and prediction can be applied using Eq. (27*). Compared to $b_1(k_g, z)$ and $b_1(k_g, t)$, the input in terms of horizontal slowness shows high quality on the convergence. Even though small dispersion still occurred at very high angle set near surface, the subtle melioration indicates that the idea of seeking for optimize prediction algorithm with a relative stationary search parameter is practicable.

Further analysis were investigated, the input $b_1(p_g, \tau)$ is shown in Figure 4d with better convergence for the completed p range, in contrast to those three inputs illustrated above. The assembling characteristic of plane wave input make it possible to delineate the lower-

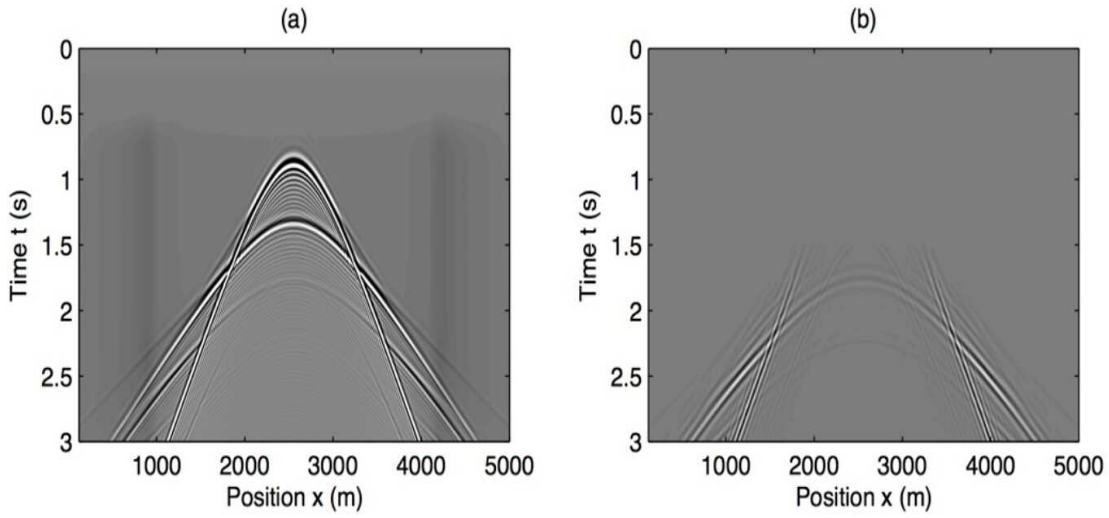

FIG. 5. Large dip artifacts caused by a fixed ϵ in (k_g, z) domain (Innanen and Pan, 2015). (a) input synthetic data acquired on a two-interface acoustic model, (b) raw prediction generated with a fixed ϵ. Large dip artifacts are visible intersecting the bottom of the panel at roughly 1km to 4km.

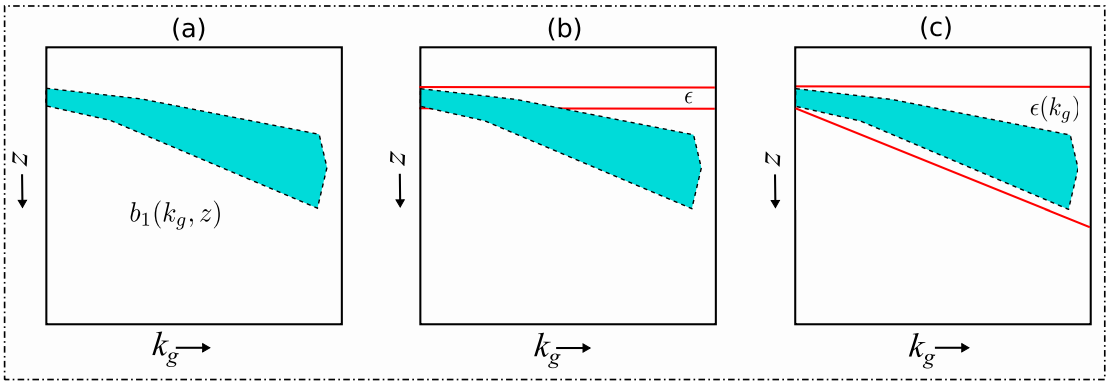

FIG. 6. Mechanism of variant search parameter in (k_g, z) domain (Innanen and Pan, 2015). (a) illustration of the input $b_1(k_g, z)$; (b) integration-limiting parameter ϵ fixed at a size appropriate to $k_g = 0$; (c) Approximate $\epsilon(k_g)$ to capture the "spread" of the sub-event.

higher-lower relationship in combination with a relative fixed ϵ. There is still room for developing a non-stationary search parameter $\epsilon(\tau)$ in $\tau - p$ domain for a complex case, especially in the range of p that interferences occurred between sub-events. One should note that the procedure of non-stationary search parameter also works in $\tau - p$ domain in a similar way, which makes plane wave algorithm to be the promising way to extend ISS-IMs prediction into 2D/3D land.

Implementation domain

However, the implementation domain remains to be another hinge, even with a non-stationary search parameter, for inverse scattering series prediction, when the preparation of input, the procedure of setup non-stationary ϵ, and time consuming come into mind. Following the illustration in the section of algorithm, inverse scattering series can be implemented in several different domains, such as (k_g, k_s, z), (k_g, k_s, t), (p_g, p_s, z), and (p_g, p_s, τ) domains. The examination of ISS-IMs prediction on post-stack data was discussed by Her-

nandez and Innanen (2014). Pan and Innanen (2015) implemented the ISS internal multiple prediction on physical modeling data in pseudo-depth domain and discussed the numerical analysis of 1.5D predicted results. Time domain prediction was introduced by Innanen (2016b,a). The plane wave domain application of ISS-IMs, first mentioned by Coates and Weglein (1996), in 1.5D case, was investigated by Sun and Innanen (2015), as well as the (p, z) prediction (Sun and Innanen, 2014). To fit the complex land, 2D ISS-IMs prediction in plane wave domain was implemented by incorporating a couple $\tau - p_g - p_s$ transform (Sun and Innanen, 2016a,b).

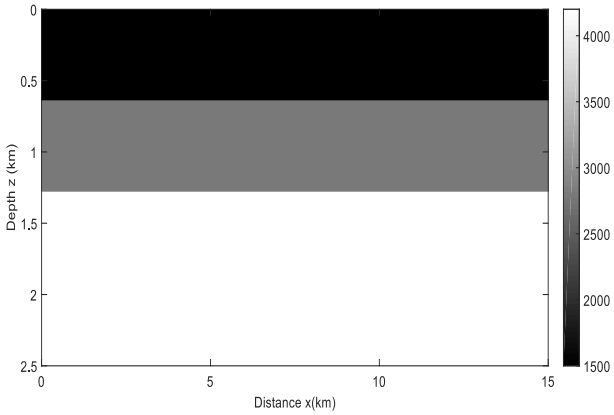

FIG. 7. Velocity model: 1500m/s (top), 2800m/s (middle), and 4200m/s (bottom).

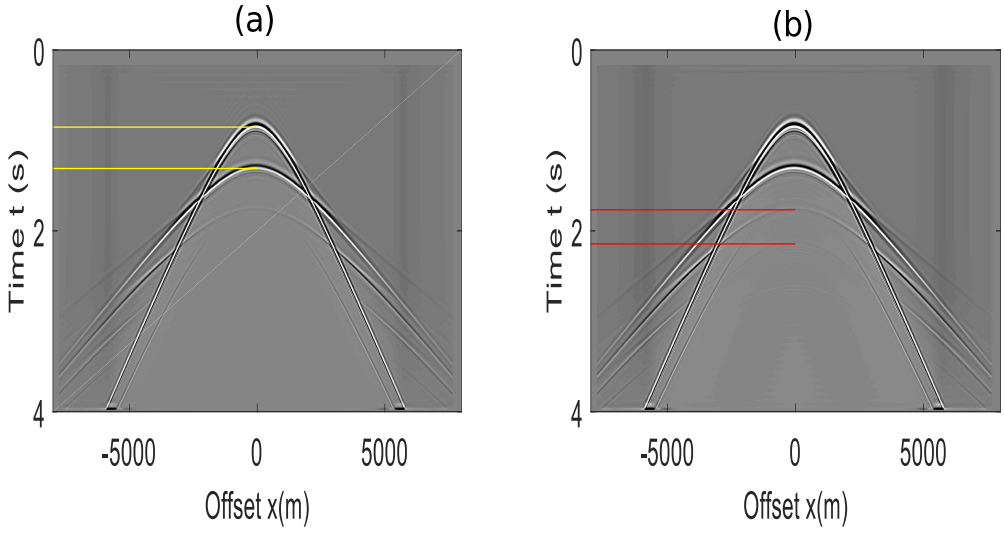

FIG. 8. Synthetic shot gather. (a) two primary events indicated, (b) 1st and 2nd order internal multiples indicated

In the following context, to investigate the affects of variant implementation domains in an institutive way, we implement the ISS-IMs prediction on a three-layer model, in (k_g, z), (p_g, z), (k_g, t), (p_g, τ) domains, respectively. Figure 7 shows the geological model with velocity varies in depth only. Velocities in top, middle and bottom are 1500m/s, 2800m/s, and 4200m/s, respectively. A single shot record of data is illustrated Figure 8, generated using the CREWES acoustic finite difference function $afd\_shortrec$, with all four boundaries set as "absorbing" to suppress the creation of free-surface multiples. Two

primaries are indicated in yellow at zero-offset traveltime (Figure 8a) and red lines denote the two-way zero offset traveltimes for 1st- and 2nd- order internal multiples, respectively (Figure 8b).

Inputs for four different domains were demonstrated in Figure 4. For (k_g, z) domain, as investigated above, a fixed search parameter could bring large dip artifacts, therefore, a wavenumber-dependent ϵ, illustrated in Figure 6, has to be applied during prediction to remove those artifacts. But, here, to show the difference between the constant $\epsilon = 0.3km$ and the wavenumber-dependent ϵ, we apply a constant ϵ in (k_g, z) domain, and apply a wavenumber-dependent $\epsilon(k_g)$ in (k_g, t) domain (Table 1). For (k_g, t) domain, limited range of integral for Eq. 30 become to $\alpha(t, t_1, \epsilon_2)$ and $\beta(t, \epsilon_1)$, which are time-variant. Similar to (k_g, z) domain, ϵ has to be wavenumber-dependent to remove large dip artifacts. Therefore, limits of integral, as the function of time and wavenumber, i.e., $\alpha(t, t_1, \epsilon_2(k_g))$ and $\beta(t, \epsilon_1(k_g))$, are accomplished in (k_g, t) domain.

Domains	Equations	Limits of integrals applied
(k_g, z)	Eq.25	$\epsilon = 0.3km$
(p_g, z)	Eq.27*	$\epsilon = 0.3km$
(k_g, t)	Eq.30	$\alpha(t, t_1, \epsilon(k_g))$ and $\beta(t, \epsilon(k_g))$
(p_g, τ)	Eq.27	$\epsilon = 0.3s$

Table 1. The corresponded limits of integrals implementing prediction in different domains, and related inputs are shown in Figure 4.

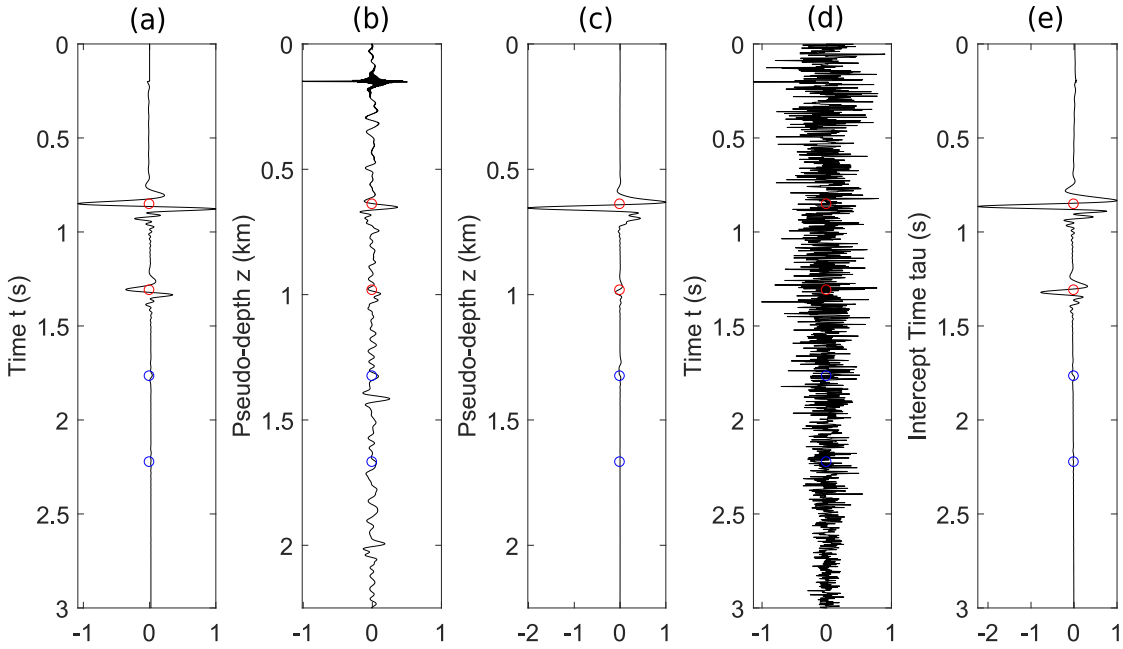

FIG. 9. Comparisons between raw trace and the stacked inputs, two-way traveltimes for primary and multiple events are indicated by red and blue dots, separately. (a) zero-offset trace, (b) input $b_1(k_g, z)$ stacked over k_g, (c) input $b_1(p_g, z)$ stacked over p_g, (d) input $b_1(k_g, t)$ stacked over k_g, (e) input $b_1(p_g, \tau)$ stacked over p_g.

For (p_g, z) and (p_g, τ) domains, a constant value, for (p_g, z), $\epsilon = 0.3km$; for (p_g, τ), $\epsilon = 0.3s$ are enforced to perform the prediction process, respectively (Table 1). The applied

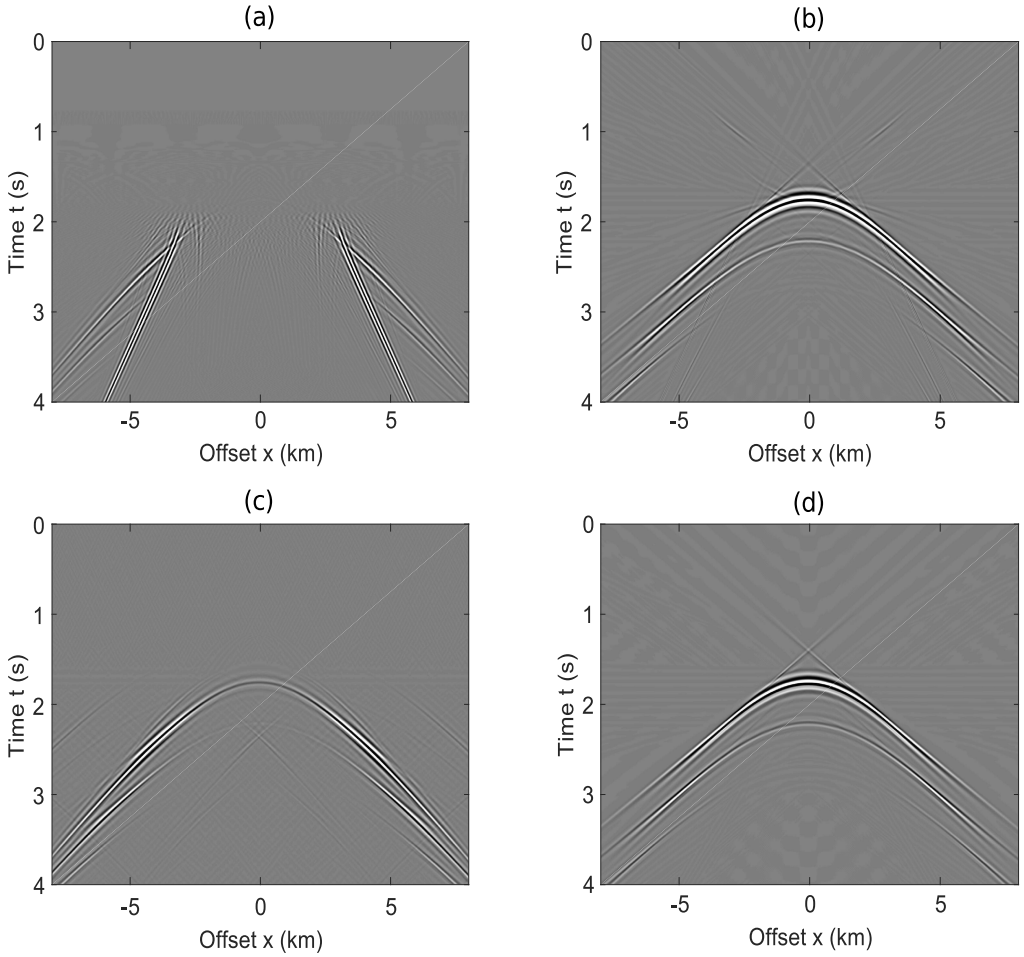

FIG. 10. The predictions of internal multiples occurred in Figure 8 using corresponded inputs shown in Figure 4. (a) predictions using input $b_1(k_g, z)$ with a constant $\epsilon = 0.3km$; (b) predictions using input $b_1(p_g, z)$ with a constant $\epsilon = 0.3km$; (c) predictions using input $b_1(k_g, t)$ with functioned limits $\alpha(t, t_1, \epsilon_2(k_g))$ and $\beta(t, \epsilon_1(k_g))$; (d) predictions using input $b_1(p_g, \tau)$ with a constant $\epsilon = 0.3s$.

integral limits in above four different domains are shown in Table 1. Again, time-offset domain is not actualized due to time consuming. Beyond that, the inputs are stacked over k_g or p_g, respectively, related to its affiliated domain, and are compared to zero-offset trace extracted from raw synthetic data. Scandalized comparisons are shown in Figure 9.

By implementing corresponded equations respectively (Table 1), predicted results for internal multiple occurred in Figure 8 can be obtained, delineated in Figure 10. As discussed before, for predictions in (k_g, z) domain with a constant ϵ value (Figure 10a), large dip artifacts occur in the results when the offset beyond the interacted point between primaries and internal multiples. Compare it to the prediction of (k_g, t) domain in Figure 10c, large dip artifacts can be reduced by applying a wavenumber-dependent search parameter. One note has to be mentioned that, compared to other three domain application, the (k_g, t) prediction process is much more time-consuming.

Comparison of inputs in (k_g, z) domain (Figure 4a) and in (p_g, z) domain (Figure 4b), it indicates that horizontal slowness has much more powerful abilities to localized the energy of events than the wavenumber. Therefore, (p_g, z) domain and (p_g, τ) domain algorithm with a constant ϵ can generate the precise prediction without introducing any large dip artifacts. Moreover, the time-variant search parameter procedure also works in (p_g, τ) domain.

CONCLUSIONS

Inverse scattering series internal multiple attenuation algorithm is a powerful and promising way to eliminate multiples on land, even though many challenges to be solved when comes in practice. In this paper, beginning with born series, we literature review the progresses, as much as we can, have been made on internal multiple prediction based on inverse scattering series since it's developed by Araujo et al. (1994) and Weglein et al. (1997). Theoretically, we investigate the mechanism of ISS-IMs attenuation algorithm both for 1D case in pseudo-depth domain, and for 2D plane wave domain, in an analogous way by analyzing the unique monotonicity relation between the real depth and intercept time.

In application, the selection of search parameter is a key characteristic to eliminate high angle artifacts and to achieve preciser prediction of internal multiple. Two way to access, (1) using a non-stationary search parameter (Innanen, 2016a), (2) implementing prediction in plane wave domain which allows a relative stationary search parameter (Sun and Innanen, 2015, 2016a,b,c) . Moreover, plane wave algorithm can also involves a non-stationary search parameter as a function of intercept time $\epsilon(\tau)$ in a similar way. One should mention that the computational burden might becomes a big challenge in a realization of time-offset domain prediction. Therefore, the plane wave domain is a more considerable option to implementing inverse scattering series internal multiple prediction on 2D/3D land data.

APPENDIX A:
Plane-Wave domain 2D ISS-IMs Prediction Algorithm

The pseudo-depth domain inverse scattering series internal multiple attenuation algorithm is legitimate only if the ordering of the real and the pseudo-depths of those sub-events are preserved (Weglein et al., 1997, 2003), which is called 'pseudo-depth monotonicity condition', written as,

$$z_1^{real} < z_2^{real} \Longleftrightarrow z_1 < z_2 \tag{A.1}$$

Here, z_1 and z_2 denote pseudo-depths, i.e., depth in reference medium.

Note that, for a plane wave propagating in a real medium, the relation between intercept time and depth can be described as,

$$\omega\tau = k_z z^{real} \tag{A.2}$$

Digging into details of Figure 2, those sub-events to reconstruct the internal multiple have in common that they shared one of the segment of upper layer ray-path. In other words, pseudo-depth domain ISS-IMs attenuation algorithm works only if the pseudo-depth has the same monotonicity condition as the real depth does for a fixed wavenumber (k_g or k_s) or horizontal slowness (p_g or p_s) related to source or receiver.

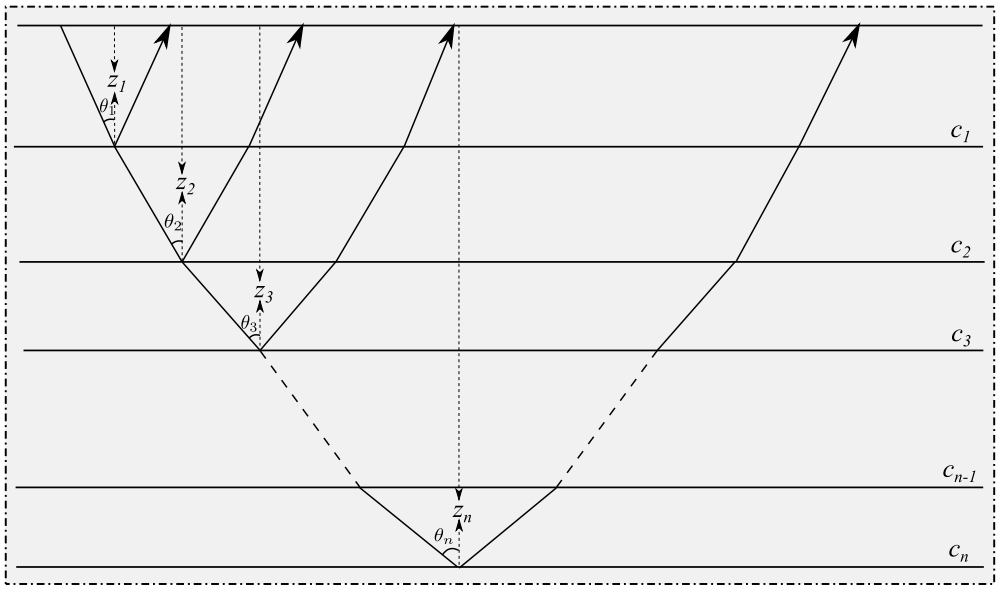

FIG. A.1. Wave propagation in n layers.

Therefore, for n-layer model (Figure A.1), Eq. (A.2) expands to n terms,

$$\begin{cases} \omega\tau_1 & = k_z^1 z_1^{real} \\ \omega(\tau_2 - \tau_1) & = k_z^2 (z_2^{real} - z_1^{real}) \\ \omega(\tau_3 - \tau_2) & = k_z^3 (z_3^{real} - z_2^{real}) \\ & \vdots \\ \omega(\tau_n - \tau_{n-1}) & = k_z^n (z_n^{real} - z_{n-1}^{real}) \end{cases} \tag{A.3}$$

where, τ_i denotes the intercept time of ray-path reflected by i^{th} scattering point, z_i^{real} represents the depth of i^{th} scattering point, and k_z^i is the vertical wavenumber of i^{th} ray-path, obtained by $k_z^i = \dfrac{\omega}{c_i}\cos\theta_i$.

Then, for $n-1$ and n layer cases, sum all equations in Eq. (A.3), we have,

$$\omega\tau_{n-1} = (k_z^1 - k_z^2)z_1^{real} + (k_z^2 - k_z^3)z_2^{real} + \cdots + (k_z^{n-2} - k_z^{n-1})z_{n-2}^{real} + k_z^{n-1}z_{n-1}^{real} \tag{A.4a}$$

$$\omega\tau_n = (k_z^1 - k_z^2)z_1^{real} + (k_z^2 - k_z^3)z_2^{real} + \cdots + (k_z^{n-1} - k_z^n)z_{n-1}^{real} + k_z^n z_n^{real} \tag{A.4b}$$

Subtracting Eq. (A.4a), for both sides, from Eq. (A.4b),

$$(\tau_n - \tau_{n-1}) = \frac{\cos\theta_n}{c_n}(z_n^{real} - z_{n-1}^{real}) \tag{A.5}$$

Eq. (A.5) indicates that, for a fixed horizontal slowness (p_g or p_s), the intercept time can be written as a monotonicity function of real depth, i.e.,

$$z_1^{real} < z_2^{real} \Longleftrightarrow \tau_1 < \tau_2 \tag{A.6}$$

Comparing Eq. (A.1) with Eq. (A.6), one can say that inverse scattering series internal multiple attenuation algorithm can also be implemented in plane wave domain.

Consider a 2D acoustic homogeneous media as background, and take Hankel transform of inverse scattering series (Eq. 18), over source and receiver coordinate (x_s and x_g),

$$\begin{aligned}
\boldsymbol{b}_1(p_g, z_g, p_s, z_s, \omega) &= \boldsymbol{G}_0(p_g, z_g, x_1, z_1, \omega)\boldsymbol{V}_1(x_1, z_1)\boldsymbol{\phi}_0(x_1, z_1, p_s, z_s, \omega) \\
\boldsymbol{0} &= \boldsymbol{G}_0(p_g, z_g, x_1, z_1, \omega)\boldsymbol{V}_2(x_1, z_1)\boldsymbol{\phi}_0(x_1, z_1, p_s, z_s, \omega) \\
&\quad + \boldsymbol{G}_0(p_g, z_g, x_1, z_1, \omega)\boldsymbol{V}_1(x_1, z_1)\boldsymbol{G}_0(x_1, z_1, x_2, z_2, \omega)\boldsymbol{V}_1(x_2, z_2)\boldsymbol{\phi}_0(x_2, z_2, p_s, z_s, \omega) \\
\boldsymbol{0} &= \boldsymbol{G}_0(p_g, z_g, x_1, z_1, \omega)\boldsymbol{V}_3(x_1, z_1)\boldsymbol{\phi}_0(x_1, z_1, p_s, z_s, \omega) \\
&\quad + \boldsymbol{G}_0(p_g, z_g, x_1, z_1, \omega)\boldsymbol{V}_2(x_1, z_1)\boldsymbol{G}_0(x_1, z_1, x_2, z_2, \omega)\boldsymbol{V}_1(x_2, z_2)\boldsymbol{\phi}_0(x_2, z_2, p_s, z_s, \omega) \\
&\quad + \boldsymbol{G}_0(p_g, z_g, x_1, z_1, \omega)\boldsymbol{V}_1(x_1, z_1)\boldsymbol{G}_0(x_1, z_1, x_2, z_2, \omega)\boldsymbol{V}_2(x_2, z_2)\boldsymbol{\phi}_0(x_2, z_2, p_s, z_s, \omega) \\
&\quad + \boldsymbol{G}_0(p_g, z_g, x_1, z_1, \omega)\boldsymbol{V}_1(x_1, z_1)\boldsymbol{G}_0(x_1, z_1, x_2, z_2, \omega)\boldsymbol{V}_1(x_2, z_2)\boldsymbol{G}_0(x_2, z_2, x_3, z_3, \omega) \\
&\quad \times \boldsymbol{V}_1(x_3, z_3)\boldsymbol{\phi}_0(x_3, z_3, p_s, z_s, \omega) \\
&\quad \vdots
\end{aligned} \tag{A.7}$$

Recall 2D Green's Function in wavenumber domain related to source and receiver locations,respectively,

$$\begin{aligned}
G_0(k_g, z_g, x_1, z_1, \omega) &= \frac{e^{-\mathrm{i}k_g x_1} e^{\mathrm{i}\nu_g |z_g - z_1|}}{\mathrm{i}2\nu_g} \\
G_0(x_1, z_1, k_s, z_s, \omega) &= \frac{e^{\mathrm{i}k_s x_1} e^{\mathrm{i}\nu_s |z_1 - z_s|}}{\mathrm{i}2\nu_s}
\end{aligned} \tag{A.8}$$

Based on Eq. (A.6), for a fixed horizontal slowness, each depth has a unique projection on intercept time. Therefore, Eq. (A.7) and Eq. (A.8) can also be re-written in $\tau - p$

dimension,

$$\begin{aligned}
\boldsymbol{b}_1(p_g,\tau_g,p_s,\tau_s,\omega) &= \boldsymbol{G}_0(p_g,\tau_g,x_1,\tau_1,\omega)\boldsymbol{V}_1(x_1,\tau_1)\boldsymbol{\phi}_0(x_1,\tau_1,p_s,\tau_s,\omega)\\
\boldsymbol{0} &= \boldsymbol{G}_0(p_g,\tau_g,x_1,\tau_1,\omega)\boldsymbol{V}_2(x_1,\tau_1)\boldsymbol{\phi}_0(x_1,\tau_1,p_s,\tau_s,\omega)\\
&\quad + \boldsymbol{G}_0(p_g,\tau_g,x_1,\tau_1,\omega)\boldsymbol{V}_1(x_1,\tau_1)\boldsymbol{G}_0(x_1,\tau_1,x_2,\tau_2,\omega)\boldsymbol{V}_1(x_2,\tau_2)\boldsymbol{\phi}_0(x_2,\tau_2,p_s,\tau_s,\omega)\\
\boldsymbol{0} &= \boldsymbol{G}_0(p_g,\tau_g,x_1,\tau_1,\omega)\boldsymbol{V}_3(x_1,\tau_1)\boldsymbol{\phi}_0(x_1,\tau_1,p_s,\tau_s,\omega)\\
&\quad + \boldsymbol{G}_0(p_g,\tau_g,x_1,\tau_1,\omega)\boldsymbol{V}_2(x_1,\tau_1)\boldsymbol{G}_0(x_1,\tau_1,x_2,\tau_2,\omega)\boldsymbol{V}_1(x_2,\tau_2)\boldsymbol{\phi}_0(x_2,\tau_2,p_s,\tau_s,\omega)\\
&\quad + \boldsymbol{G}_0(p_g,\tau_g,x_1,\tau_1,\omega)\boldsymbol{V}_1(x_1,\tau_1)\boldsymbol{G}_0(x_1,\tau_1,x_2,\tau_2,\omega)\boldsymbol{V}_2(x_2,\tau_2)\boldsymbol{\phi}_0(x_2,\tau_2,p_s,\tau_s,\omega)\\
&\quad + \boldsymbol{G}_0(p_g,\tau_g,x_1,\tau_1,\omega)\boldsymbol{V}_1(x_1,\tau_1)\boldsymbol{G}_0(x_1,\tau_1,x_2,\tau_2,\omega)\boldsymbol{V}_1(x_2,\tau_2)\boldsymbol{G}_0(x_2,\tau_2,x_3,\tau_3,\omega)\\
&\quad \times \boldsymbol{V}_1(x_3,\tau_3)\boldsymbol{\phi}_0(x_3,\tau_3,p_s,\tau_s,\omega)\\
&\quad \vdots
\end{aligned} \tag{A.9}$$

And Green's Function in terms of horizontal slowness p,

$$\begin{aligned}
\boldsymbol{G}_0(p_g,\tau_g,x_1,\tau_1,\omega) &= \frac{e^{-\mathrm{i}p_g x_1}e^{\mathrm{i}\omega|\tau_g-\tau_{1s}|}}{\mathrm{i}2\omega q_g}\\
\boldsymbol{G}_0(x_1,\tau_1,p_s,\tau_s,\omega) &= \frac{e^{\mathrm{i}p_s x_1}e^{\mathrm{i}\omega|\tau_{1g}-\tau_s|}}{\mathrm{i}2\omega q_s}
\end{aligned} \tag{A.10}$$

Here, q_g and q_s are vertical slowness with respect to receiver and source location. τ_g and τ_s are one-way vertical travel time corresponded to receiver and source side.

Substituting plane wave domain Green's Function into first equation of Eq. (A.9),

$$\begin{aligned}
b_1(p_g,\tau_g,p_s,\tau_s,\omega) &= \iint_{-\infty}^{+\infty} \boldsymbol{G}_0(p_g,\tau_g,x_1,\tau_1,\omega)V_1(x_1,\tau_1)\phi_0(x_1,\tau_1,p_s,\tau_s,\omega)\mathrm{d}x_1\mathrm{d}\tau_1\\
&= \iint_{-\infty}^{+\infty} \frac{e^{-\mathrm{i}p_g x_1}e^{\mathrm{i}\omega|\tau_g-\tau_{1s}|/2}}{\mathrm{i}2\omega q_g}V_1(x_1,\tau_1)e^{\mathrm{i}p_s x_1}e^{\mathrm{i}\omega|\tau_{1g}-\tau_s|/2}\mathrm{d}x_1\mathrm{d}\tau_1\\
&= \frac{e^{-\mathrm{i}\omega(\tau_s+\tau_g)}}{\mathrm{i}2\omega q_g}\iint_{-\infty}^{+\infty} e^{\mathrm{i}(p_s-p_g)x_1}e^{\mathrm{i}\omega\tau_1}V_1(x_1,\tau_1)\mathrm{d}x_1\mathrm{d}\tau_1\\
&= \frac{e^{-\mathrm{i}\omega(\tau_s+\tau_g)}}{\mathrm{i}2\omega q_g}V_1(p_s-p_g,\omega|\tau_1)
\end{aligned} \tag{A.11}$$

Then, the 1st-order of scattering potential can be written as,

$$V_1(p_s-p_g,\omega|\tau_1) = \mathrm{i}2\omega q_g e^{\mathrm{i}\omega(\tau_s+\tau_g)}b_1(p_g,p_s,\omega|\tau_1) \tag{A.12}$$

Similarly, all first order internal multiples are related to the 3rd-order of inverse scatter-

ing series when longer-shorter-longer criterion is satisfied,

$$
\begin{aligned}
&W_{33}(p_g,\tau_g,p_s,\tau_s,\omega)\\
&=-\iint_{-\infty}^{+\infty} G_0(p_g,\tau_g,x_1,\tau_1)V_1(x_1,\tau_1)\mathrm{d}x_1\mathrm{d}\tau_1 \iint_{-\infty}^{\tau_1} G_0(x_1,\tau_1,x_2,\tau_2)V_1(x_2,\tau_2)\mathrm{d}x_2\mathrm{d}\tau_2\\
&\quad\times\iint_{\tau_2}^{+\infty} G_0(x_2,\tau_2,x_3,\tau_3)V_1(x_3,\tau_3)\boldsymbol{\phi}_0(x_3,\tau_3,p_s,\tau_s,\omega)\mathrm{d}x_3\mathrm{d}\tau_3\\
&=-\iint_{-\infty}^{+\infty} G_0(p_g,\tau_g,x_1,\tau_1)V_1(x_1,\tau_1)\mathrm{d}x_1\mathrm{d}\tau_1\\
&\quad\times\iint_{-\infty}^{\tau_1}\left[\frac{1}{2\pi}\int_{-\infty}^{+\infty} e^{\mathrm{i}p_1x_1}G_0(p_1,\tau_1,x_2,\tau_2)\mathrm{d}p_1\right]V_1(x_2,\tau_2)\mathrm{d}x_2\mathrm{d}\tau_2\\
&\quad\times\iint_{\tau_2}^{+\infty}\left[\frac{1}{2\pi}\int_{-\infty}^{+\infty} e^{\mathrm{i}p_2x_2}G_0(p_2,\tau_2,x_3,\tau_3)\mathrm{d}p_2\right]V_1(x_3,\tau_3)\boldsymbol{\phi}_0(x_3,\tau_3,p_s,\tau_s,\omega)\mathrm{d}x_3\mathrm{d}\tau_3\\
&=-\frac{1}{(2\pi)^2}\iint_{-\infty}^{+\infty}\mathrm{d}p_1\mathrm{d}p_2\iint_{-\infty}^{+\infty}\mathrm{d}x_1\mathrm{d}\tau_1\frac{e^{-\mathrm{i}p_gx_1}e^{\mathrm{i}\omega|\tau_g-\tau_{1s}|}}{\mathrm{i}2\omega q_g}V_1(x_1,\tau_1)\\
&\quad\times\iint_{-\infty}^{\tau_1}\mathrm{d}x_2\mathrm{d}\tau_2\frac{e^{\mathrm{i}p_1(x_1-x_2)}e^{\mathrm{i}\omega|\tau_{1g}-\tau_{2s}|}}{\mathrm{i}2\omega q_1}V_1(x_2,\tau_2)\\
&\quad\times\iint_{\tau_2}^{+\infty}\mathrm{d}x_3\mathrm{d}\tau_3\frac{e^{\mathrm{i}p_2(x_2-x_3)}e^{\mathrm{i}\omega|\tau_{2g}-\tau_{3s}|}}{\mathrm{i}2\omega q_2}V_1(x_3,\tau_3)e^{\mathrm{i}p_sx_3}e^{\mathrm{i}\omega|\tau_{3g}-\tau_s|}\\
&=-\frac{1}{(2\pi)^2}\iint_{-\infty}^{+\infty}\mathrm{d}p_1\mathrm{d}p_2\frac{e^{-\mathrm{i}\omega(\tau_s+\tau_g)}}{(\mathrm{i}2\omega q_g)(\mathrm{i}2\omega q_1)(\mathrm{i}2\omega q_2)}\iint_{-\infty}^{+\infty}e^{\mathrm{i}(p_1-p_g)x_1}e^{\mathrm{i}\omega\tau_1}V_1(x_1,\tau_1)\mathrm{d}x_1\mathrm{d}\tau_1\\
&\quad\times\iint_{-\infty}^{\tau_1}e^{\mathrm{i}(p_2-p_1)x_2}e^{-\mathrm{i}\omega\tau_2}V_1(x_2,\tau_2)\mathrm{d}x_2\mathrm{d}\tau_2\iint_{\tau_2}^{+\infty}e^{\mathrm{i}(p_s-p_2)x_3}e^{\mathrm{i}\omega\tau_3}V_1(x_3,\tau_3)\mathrm{d}x_3\mathrm{d}\tau_3\\
&=-\frac{1}{(2\pi)^2}\iint_{-\infty}^{+\infty}\mathrm{d}p_1\mathrm{d}p_2\frac{e^{-\mathrm{i}\omega(\tau_s+\tau_g)}}{(\mathrm{i}2\omega q_g)(\mathrm{i}2\omega q_1)(\mathrm{i}2\omega q_2)}\\
&\quad\times V_1(p_1-p_g,\omega|\tau_1)V_1(p_2-p_1,-\omega|\tau_2<\tau_1)V_1(p_s-p_2,\omega|\tau_3>\tau_2)
\end{aligned}
\tag{A.13}
$$

Replacing scattering potential by the weighted data, we have,

$$
\begin{aligned}
W_{33}(p_g,\tau_g,p_s,\tau_s,\omega)=&-\frac{1}{(2\pi)^2}\iint_{-\infty}^{+\infty}\mathrm{d}p_1\mathrm{d}p_2e^{\mathrm{i}\omega(\tau_{1s}-\tau_{1g})}e^{\mathrm{i}\omega(\tau_{2g}-\tau_{2s})}\boldsymbol{b}_1(p_g,p_1,\omega|\tau_1)\\
&\times\boldsymbol{b}_1(p_1,p_2,-\omega|\tau_2<\tau_1)\boldsymbol{b}_1(p_2,p_s,\omega|\tau_3>\tau_2)
\end{aligned}
\tag{A.14}
$$

Inverse Fourier transform of $b_1(p_g,p_s,\omega)$ over instantaneous frequency ω, all first-order internal multiples can be obtained,

$$
\begin{aligned}
b_3(p_g,p_s,\omega)=&-\frac{1}{(2\pi)^2}\iint_{-\infty}^{+\infty}\mathrm{d}p_1\mathrm{d}p_2e^{\mathrm{i}\omega(\tau_{1s}-\tau_{1g})}e^{\mathrm{i}\omega(\tau_{2g}-\tau_{2s})}\int_{-\infty}^{+\infty}\mathrm{d}\tau_1e^{\mathrm{i}\omega\tau_1}\boldsymbol{b}_1(p_g,p_1,\tau_1)\\
&\times\int_{-\infty}^{\tau_1}\mathrm{d}\tau_2e^{-\mathrm{i}\omega\tau_2}\boldsymbol{b}_1(p_1,p_2,\tau_2)\int_{\tau_2}^{+\infty}\mathrm{d}\tau_3e^{\mathrm{i}\omega\tau_3}\boldsymbol{b}_1(p_2,p_s,\tau_3)
\end{aligned}
\tag{A.15}
$$

Similarly, at least 5 perturbations have to be existed to generate 2nd-order internal multiple satisfying longer-shorter-longer-shorter-longer relationship, based on Eq.(A.14), we have,

$$\begin{aligned} b_5(p_g,p_s,\omega) = -\frac{1}{(2\pi)^4}\int_{-\infty}^{+\infty} \mathrm{d}p_1 e^{\mathrm{i}\omega(\tau_{1s}-\tau_{1g})} b_1(p_g,p_1,\omega|\tau_1) \\ \times \int_{-\infty}^{+\infty} \mathrm{d}p_2 e^{-\mathrm{i}\omega(\tau_{2s}-\tau_{2g})} b_1(p_1,p_2,-\omega|\tau_2<\tau_1) \\ \times \int_{-\infty}^{+\infty} \mathrm{d}p_3 e^{\mathrm{i}\omega(\tau_{3s}-\tau_{3g})} b_1(p_2,p_3,\omega|\tau_3>\tau_2) \\ \times \int_{-\infty}^{+\infty} \mathrm{d}p_4 e^{\mathrm{i}-\omega(\tau_{4s}-\tau_{4g})} b_1(p_3,p_4,-\omega|\tau_4<\tau_3) \\ \times b_1(p_4,p_s,\omega|\tau_5>\tau_4) \end{aligned} \tag{A.16}$$

Rewrite Eq.(A.14) and Eq.(A.16) as,

$$\begin{aligned} b_3(p_g,p_s,\omega) &= -\frac{1}{(2\pi)^2}\int_{-\infty}^{+\infty} \mathrm{d}p_1 e^{\mathrm{i}\omega(\tau_{1s}-\tau_{1g})} b_1(p_g,p_1,\omega|\tau_1) A_3(p_1,p_s,\omega|\tau_1) \\ b_5(p_g,p_s,\omega) &= -\frac{1}{(2\pi)^4}\int_{-\infty}^{+\infty} \mathrm{d}p_1 e^{\mathrm{i}\omega(\tau_{1s}-\tau_{1g})} b_1(p_g,p_1,\omega|\tau_1) A_5(p_1,p_s,\omega|\tau_1) \end{aligned} \tag{A.17}$$

Here,

$$\begin{aligned} A_3(p_1,p_s,\omega|\tau_1) &= \int_{-\infty}^{+\infty} \mathrm{d}p_2 e^{-\mathrm{i}\omega(\tau_{2s}-\tau_{2g})} b_1(p_1,p_2,-\omega|\tau_2<\tau_1) b_1(p_2,p_s,\omega|\tau_3>\tau_2) \\ A_5(p_1,p_s,\omega|\tau_1) &= \int_{-\infty}^{+\infty} \mathrm{d}p_2 e^{-\mathrm{i}\omega(\tau_{2s}-\tau_{2g})} b_1(p_1,p_2,-\omega|\tau_2<\tau_1) \\ &\times \int_{-\infty}^{+\infty} \mathrm{d}p_3 e^{\mathrm{i}\omega(\tau_{3s}-\tau_{3g})} b_1(p_2,p_3,\omega|\tau_3>\tau_2) \\ &\times \int_{-\infty}^{+\infty} \mathrm{d}p_4 e^{\mathrm{i}-\omega(\tau_{4s}-\tau_{4g})} b_1(p_3,p_4,-\omega|\tau_4<\tau_3) \\ &\times b_1(p_4,p_s,\omega|\tau_5>\tau_4) \\ &= \int_{-\infty}^{+\infty} \mathrm{d}p_2 e^{-\mathrm{i}\omega(\tau_{2s}-\tau_{2g})} b_1(p_1,p_2,-\omega|\tau_2<\tau_1) \\ &\times \int_{-\infty}^{+\infty} \mathrm{d}p_3 e^{\mathrm{i}\omega(\tau_{3s}-\tau_{3g})} b_1(p_2,p_3,\omega|\tau_3>\tau_2) \\ &\times A_3(p_3,p_s,\omega|\tau_3) \end{aligned} \tag{A.18}$$

By that analogy, for nth-order internal multiple, attenuation algorithm can be expressed as,

$$b_{2n+1}(p_g,p_s,\omega) = -\frac{1}{(2\pi)^2}\int_{-\infty}^{+\infty} \mathrm{d}p_1 e^{\mathrm{i}\omega(\tau_{1s}-\tau_{1g})} b_1(p_g,p_1,\omega|\tau_1) A_{2n+1}(p_1,p_s,\omega|\tau_1) \qquad n=1,2,3,... \tag{A.19}$$

with,

$$A_{2n+1}(p_1,p_s,\omega|\tau_1)=\int_{-\infty}^{+\infty}\mathrm{d}p_2 e^{-\mathrm{i}\omega(\tau_{2s}-\tau_{2g})}\boldsymbol{b}_1(p_1,p_2,-\omega|\tau_2<\tau_1)$$
$$\times\int_{-\infty}^{+\infty}\mathrm{d}p_3 e^{\mathrm{i}\omega(\tau_{3s}-\tau_{3g})}\boldsymbol{b}_1(p_2,p_3,\omega|\tau_3>\tau_2)A_{2n-1}(p_1,p_s,\omega|\tau_1)$$
$$n=1,2,3,... \tag{A.20}$$

Take inverse Fourier transform angular frequency ω,

$$b_{2n+1}(p_g,p_s,\omega)=-\frac{1}{(2\pi)^{2n}}\iint_{-\infty}^{+\infty}\mathrm{d}p_1\mathrm{d}\tau_1 e^{\mathrm{i}\omega(\tau_{1s}-\tau_{1g})}e^{\mathrm{i}\omega\tau_1}\boldsymbol{b}_1(p_g,p_1,\tau_1)A_{2n+1}(p_1,p_s,\tau_1)$$
$$n=1,2,3,... \tag{A.21}$$

With,

$$A_3(p_1,p_s,\tau_1)=\int_{-\infty}^{+\infty}\mathrm{d}p_2 e^{-\mathrm{i}\omega(\tau_{2s}-\tau_{2g})}\int_{-\infty}^{\tau_1}\mathrm{d}\tau_2 e^{-\mathrm{i}\omega\tau_2}\boldsymbol{b}_1(p_1,p_2,\tau_2)$$
$$\times\int_{\tau_2}^{+\infty}\mathrm{d}\tau_3 e^{\mathrm{i}\omega\tau_3}\boldsymbol{b}_1(p_2,p_s,\tau_3),$$
$$A_{2n+1}(p_1,p_s,\tau_1)=\int_{-\infty}^{+\infty}\mathrm{d}p_2 e^{-\mathrm{i}\omega(\tau_{2s}-\tau_{2g})}\int_{-\infty}^{\tau_1}\mathrm{d}\tau_2 e^{-\mathrm{i}\omega\tau_2}\boldsymbol{b}_1(p_1,p_2,\tau_2)$$
$$\times\int_{-\infty}^{+\infty}\mathrm{d}p_3 e^{\mathrm{i}\omega(\tau_{3s}-\tau_{3g})}\int_{\tau_2}^{+\infty}\mathrm{d}\tau_3 e^{\mathrm{i}\omega\tau_3}\boldsymbol{b}_1(p_2,p_3,\tau_3)$$
$$\times A_{2n-1}(p_3,p_s,\tau_3),\qquad n=2,3,4,... \tag{A.22}$$

REFERENCES

Araujo, F. V., Weglein, A. B., Carvalho, P. M., and Stolt, R., 1994, Inverse scattering series for multiple attenuation: An example with surface and internal multiples, Tech. rep., Society of Exploration Geophysicists, Tulsa, OK (United States).

Berkhout, A., 2006, Seismic processing in the inverse data space: Geophysics, **71**, No. 4, A29–A33.

Berkhout, A., and Verschuur, D., 2005, Removal of internal multiples with the common-focus-point (cfp) approach: Part 1âĂŤexplanation of the theory: Geophysics, **70**, No. 3, V45–V60.

Coates, R., and Weglein, A., 1996, Internal multiple attenuation using inverse scattering: Results from prestack 1 & 2d acoustic and elastic synthetics, *in* 1996 SEG Annual Meeting, Society of Exploration Geophysicists.

de Melo, F. X., Idris, M., Wu, Z. J., Kostov, C. et al., 2014, Cascaded internal multiple attenuation with inverse scattering series: Western canada case study, *in* 2014 SEG Annual Meeting, Society of Exploration Geophysicists.

Hernandez, M., and Innanen, K. A. H., 2014, Identifying internal multiples using 1d prediction: Physical modelling and land data examples: Canadian journal of exploration geophysics, **39**, No. 1, 37–47.

Innanen, K. A. H., 2016a, Time and offset domain internal multiple prediction with nonstationary parameters, *in* SEG Technical Program Expanded Abstracts 2016, Society of Exploration Geophysicists, 4518–4523.

Innanen, K. A. H., 2016b, Time domain internal multiple prediction: CSEG Geoconvention.

Innanen, K. A. H., and Pan, P., 2015, Large dip artifacts in 1.5d internal multiple prediction and their mitigation: CSEG Geoconvention.

Kelamis, P., Erickson, K., Burnstad, R., Clark, R., and Verschuur, D., 2002a, Data-driven internal multiple attenuationâĂŤapplications and issues on land data: Soc. of Expl. Geophys, 2035–2038.

Kelamis, P. G., Erickson, K. E., Verschuur, D. J., and Berkhout, A., 2002b, Velocity-independent redatuming: A new approach to the near-surface problem in land seismic data processing: The Leading Edge, **21**, No. 8, 730–735.

Liu, F., Sen, M. K., and Stoffa, P. L., 2000, Dip selective 2-d multiple attenuation in the plane-wave domain: Geophysics, **65**, No. 1, 264–274.

Luo, Y., Kelamis, P. G., Fu, Q., Huo, S., Sindi, G., Hsu, S.-Y., and Weglein, A. B., 2011, Elimination of land internal multiples based on the inverse scattering series: The Leading Edge, **30**, No. 8, 884–889.

Luo, Y., Zhu, W., Kelamis, P. G. et al., 2007, Internal multiple reduction in inverse-data domain: SEG Expanded Abstracts. San Antonio:[sn], 125–129.

Ma, J., Sen, M. K., and Chen, X., 2009, Free-surface multiple attenuation using inverse data processing in the coupled plane-wave domain: Geophysics, **74**, No. 4, V75–V81.

Nita, B. G., and Weglein, A. B., 2009, Pseudo-depth/intercept-time monotonicity requirements in the inverse scattering algorithm for predicting internal multiple reflections: Communications in Computational Physics, **5**, No. 1, 163.

Pan, P., 2015, 1.5 d internal multiple prediction: an application on synthetic data, physical modelling data and land data synthetics: M.Sc. thesis, University of Calgary.

Pan, P., and Innanen, K. A. H., 2015, 1.5d internal multiple prediction on physical modeling data: CSEG Geoconvention.

Pan, P., Innanen, K. A. H. et al., 2014, Numerical analysis of 1.5 d internal multiple prediction, *in* 2014 SEG Annual Meeting, Society of Exploration Geophysicists.

Sun, J., and Innanen, K., 2016a, Interbed multiple prediction on land: which technology, and which domain?: CSEG Recorder, **41**, No. 10, 24–29.

Sun, J., and Innanen, K. A. H., 2014, 1.5d internal multiple prediction in the plane wave domain: CREWES Research Report, **26**, 1–11.

Sun, J., and Innanen, K. A. H., 2015, 1.5 d internal multiple prediction in the plane wave domain: CSEG Geoconvention.

Sun, J., and Innanen, K. A. H., 2016b, Extension of internal multiple prediction: 1.5 d to 2d in double plane wave domain: CSEG Geoconvention.

Sun, J., and Innanen, K. A. H., 2016c, Inverse-scattering series internal-multiple prediction in the double plane-wave domain, *in* SEG Technical Program Expanded Abstracts 2016, Society of Exploration Geophysicists, 4555–4560.

Taner, M., 1980, Long period sea-floor multiples and their suppression: Geophysical Prospecting, **28**, No. 1, 30–48.

Verschuur, D. J., 1991, Surface-related multiple elimination, an inversion approach: Ph.D. thesis, Technische Univ., Delft (Netherlands).

Weglein, A. B., Araújo, F. V., Carvalho, P. M., Stolt, R. H., Matson, K. H., Coates, R. T., Corrigan, D., Foster, D. J., Shaw, S. A., and Zhang, H., 2003, Inverse scattering series and seismic exploration: Inverse problems, **19**, No. 6, R27.

Weglein, A. B., Gasparotto, F. A., Carvalho, P. M., and Stolt, R. H., 1997, An inverse-scattering series method for attenuating multiples in seismic reflection data: Geophysics, **62**, No. 6, 1975–1989.

Weglein, A. B., and Matson, K. H., 1998, Inverse scattering internal multiple attenuation: An analytic example and subevent interpretation, *in* SPIE's International Symposium on Optical Science, Engineering, and Instrumentation, International Society for Optics and Photonics, 108–117.

Wu, Z. J., Dragoset, B. et al., 2011, Robust internal multiple prediction algorithm, *in* 2011 SEG Annual Meeting, Society of Exploration Geophysicists.

Zou, Y., and Weglein, A. B., 2015, An internal-multiple elimination algorithm for all first-order internal multiples for a 1d earth, *in* 2015 SEG Annual Meeting, Society of Exploration Geophysicists.